Supplementary materials

Synthesis, Structure, and Magnetic Properties of Linear Trinuclear Cu^{II} and Ni^{II} Complexes of Porphyrin Analogues Embedded with Binaphthol Units

Jun-ichiro Setsune*, Shintaro Omae, Yukinori Tsujimura, Tomoyuki Mochida, Takahiro Sakurai, and Hitoshi Ohta

NMR spectra

Figure S1: ^{1}H NMR spectra of (*S*)-3,3′-bis(5-carboethoxy-4-ethyl-3-methyl-2-pyrryl)-1,1′-bi-2-naphthol ((*S*)-**2a**) and (*S*)-3,3′-bis(5-carboethoxy-3,4- diethyl-2-pyrryl)-1,1′-bi-2-naphthol ((*S*)-**2b**).

Figure S2: ^{1}H NMR spectra of (*S*)-3,3′-bis(4-ethyl-3-methyl-2-pyrryl)-1,1′-bi-2-naphthol ((*S*)-**3a**) and (*S*)-3,3′-bis(3,4-diethyl-2-pyrryl)-1,1′-bi-2-naphthol ((*S*)-**3b**).

Figure S3: ^{1}H NMR spectra of the bis(binaphthol)tetrapyrrole (*S*)-**4a** and (*S*)-**4b**.

Figure S4: Variable temperature ^{1}H NMR spectra of the Cu_3 complex of bis(binaphthol)tetrapyrrole ((*S*)-**5a**).

Figure S5: Variable temperature ^{1}H NMR spectra of the Cu_3 complex of bis(binaphthol)tetrapyrrole ((*S*)-**5b**).

Figure S6: Variable temperature ^{1}H NMR spectra of the Ni_3 complex of bis(binaphthol)tetrapyrrole ((*S*)-**6a**).

Figure S7: Variable temperature ^{1}H NMR spectra of the Ni_3 complex of bis(binaphthol)tetrapyrrole ((*S*)-**6b**).

Figure S8: 2D COSY spectrum of the Cu_3 complex of bis(binaphthol)tetrapyrrole ((*S*)-**5a**) at 313 K.

Figure S9: 2D COSY spectrum of the Ni_3 complex of bis(binaphthol)tetrapyrrole ((*S*)-**6a**) at 293 K.

UV-Vis and CD spectra

Figure S10: CD spectra of (*R*)-**4a** and (*S*)-**4a** in CH_2Cl_2 and their HPLC traces on chiral column.

Figure S11: CD and UV-Vis spectral changes of (*S*)-**5a** upon addition of butylamine in CH_2Cl_2.

Figure S12: CD and UV-Vis spectral changes of (*S*)-**6a** in CH_2Cl_2 upon addition of butylamine.

X-ray and DFT data

Table S1: Cu-to-H distances (Å) in the X-ray structure of (*S*)-**5a**.

Table S2**:** Structural data (distance (Å) and angle (°)) of the Cu_3O_4 core of (*S*)-**5a** obtained by X-ray crystallography and theoretical DFT calculations.

Figure S13: DFT-calculated structure of (*S*)-**5a** of doublet (top) and quartet (bottom) using B3LYP functional (left) and wB97XD functional (right).

Table S3: Spin density of (*S*)-**5a** calculated by DFT (6-31G(d), LANL2DZ/ωB97XD).

Table S4**:** Spin density of (*S*)-**5a** calculated by DFT (6-31G(d), LANL2DZ/B3LYP).

NMR spectra

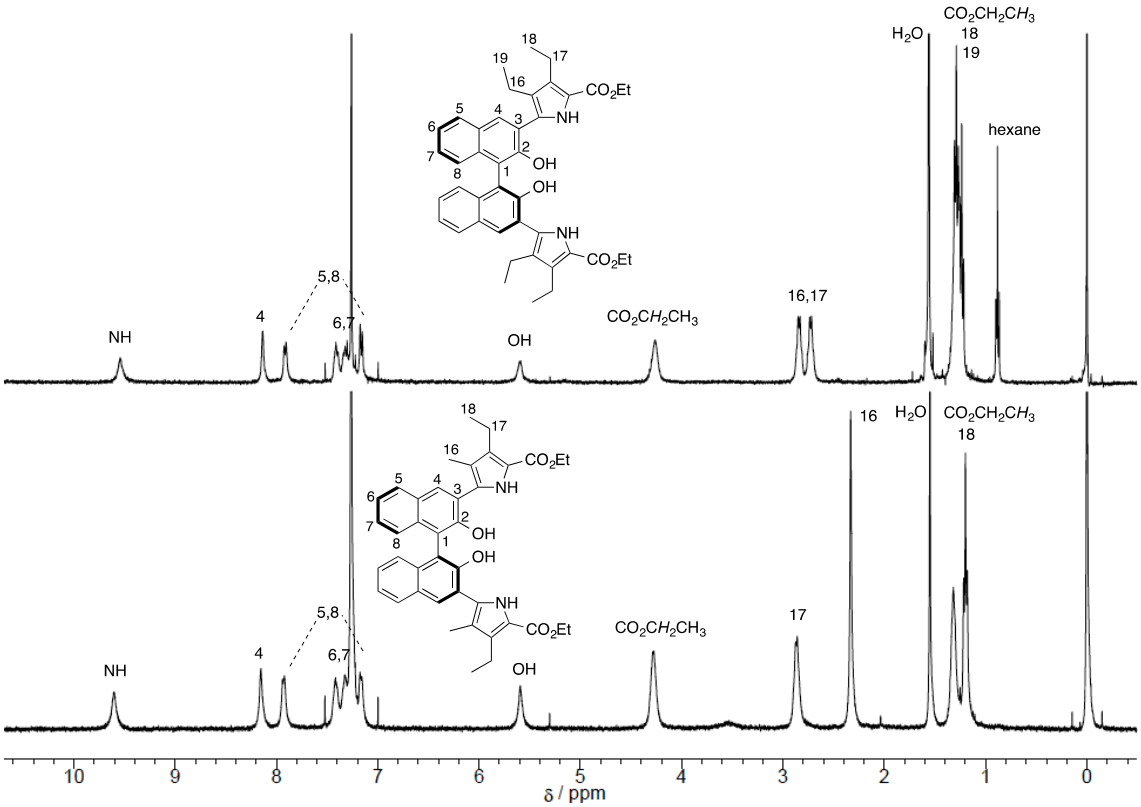

Figure S1. ^{1}H NMR spectra of (*S*)-3,3′-bis(5-carboethoxy-4-ethyl-3-methyl-2-pyrryl)-1,1′-bi-2-naphthol ((*S*)-**2a**) (bottom) and (*S*)-3,3′-bis(5-carboethoxy-3,4-diethyl-2-pyrryl)-1,1′-bi-2-naphthol ((*S*)-**2b**) (top). Signals at 1.55 ppm and 0.88 ppm are due to water and hexane.

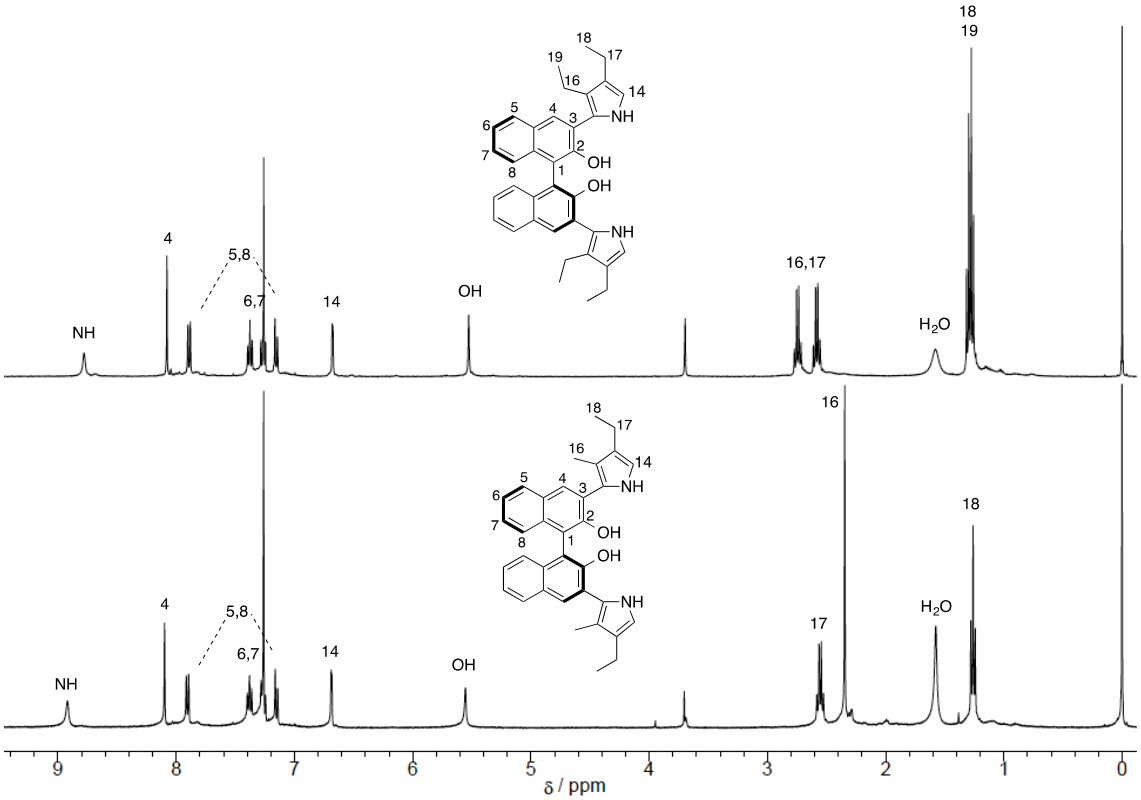

Figure S2. ^{1}H NMR spectra of (*S*)-3,3′-bis(4-ethyl-3-methyl-2-pyrryl)-1,1′-bi-2- naphthol ((*S*)-**3a**) (bottom) and (*S*)-3,3′-bis(3,4-diethyl-2-pyrryl)-1,1′-bi-2- naphthol ((*S*)-**3b**) (top). A broad signal at 1.6 ppm (water) and signals at 3.76 (impurity) are seen.

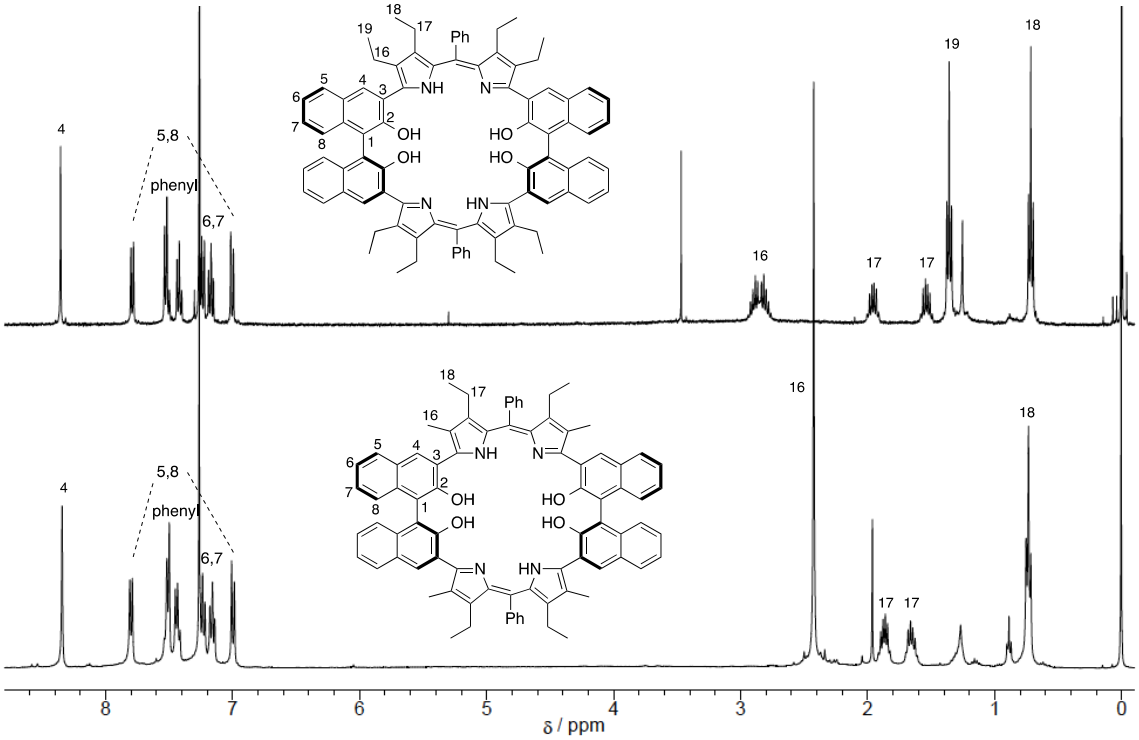

Figure S3. ^{1}H NMR spectra of the bis(binaphthol)tetrapyrrole (*S*)-**4a** (bottom) and (*S*)-**4b** (top). Signals at 0.89 ppm and 1.27 ppm are due to hexane and singlet at 1.97 ppm (impurity) is seen (bottom); signals at 3.47 ppm (methanol) and 1.25 ppm (impurity) are seen (top).

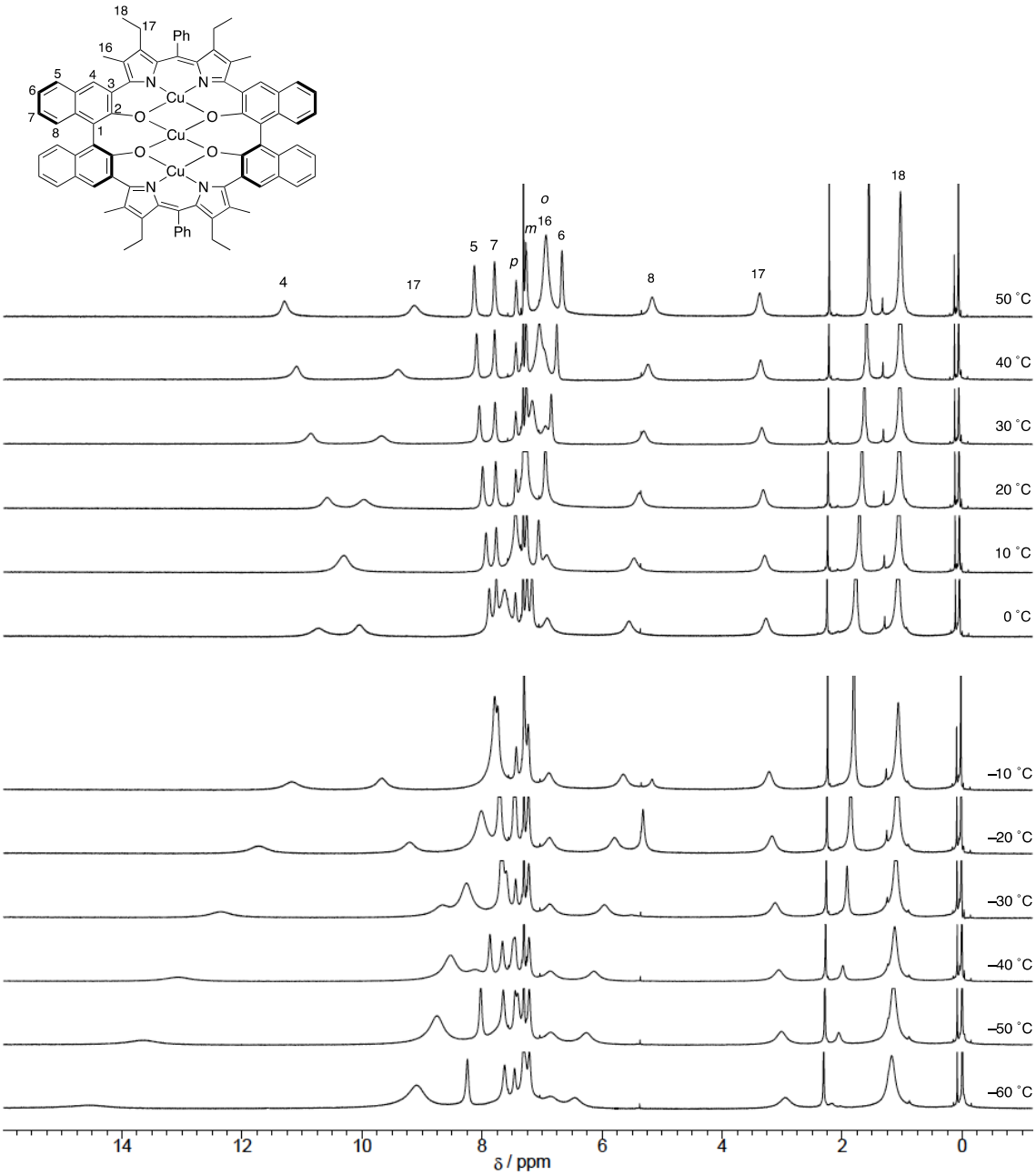

Figure S4. Variable temperature ^{1}H NMR spectra of the Cu_3 complex of bis(binaphthol)tetrapyrrole ((*S*)-**5a**). 50 ˚C ~ 0 ˚C (top) and –10 ˚C ~ –60 ˚C (bottom).

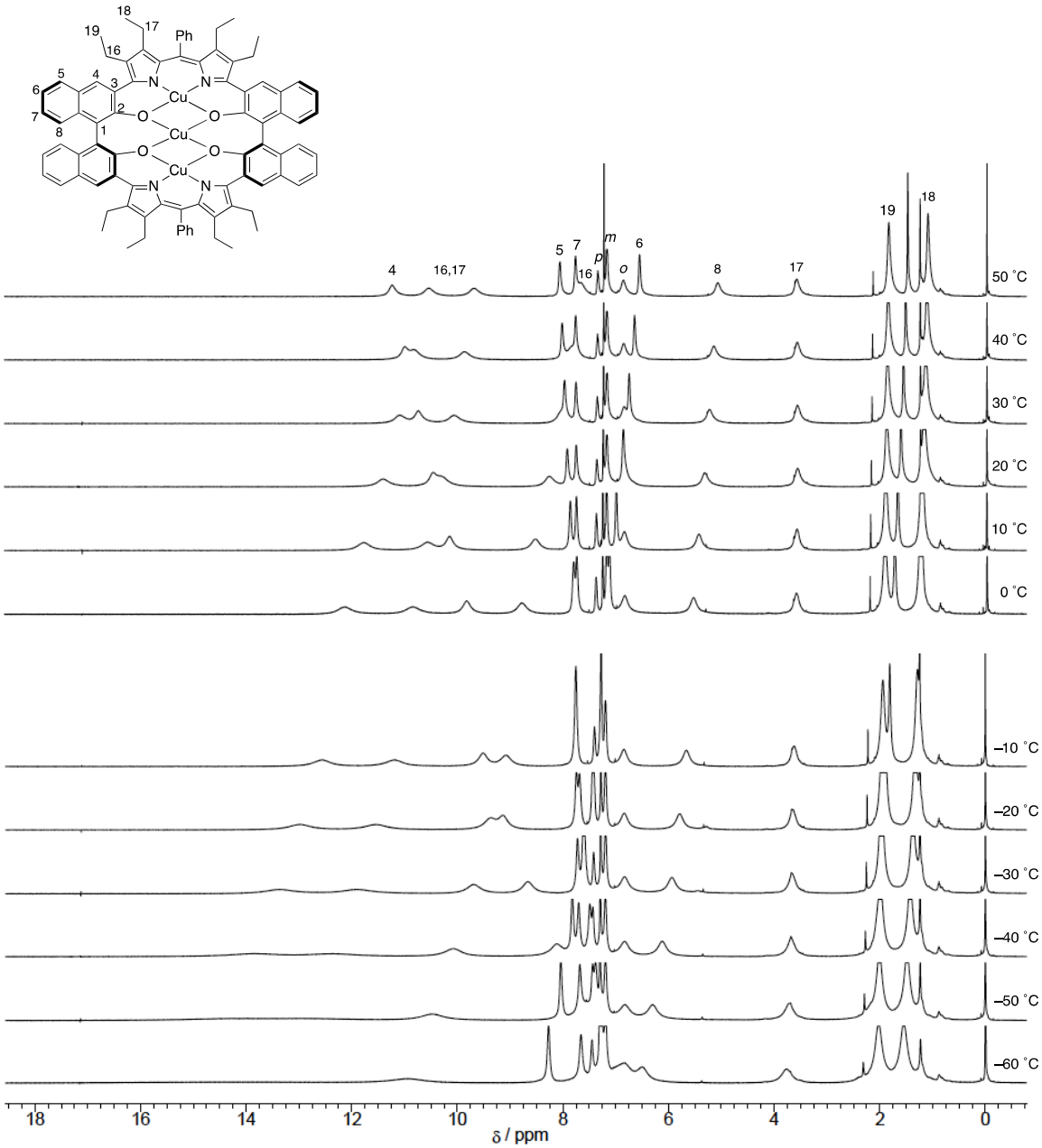

Figure S5. Variable temperature ^{1}H NMR spectra of the Cu_3 complex of bis(binaphthol)tetrapyrrole ((*S*)-**5b**). 50 ˚C ~ 0 ˚C (top) and –10 ˚C ~ –60 ˚C (bottom).

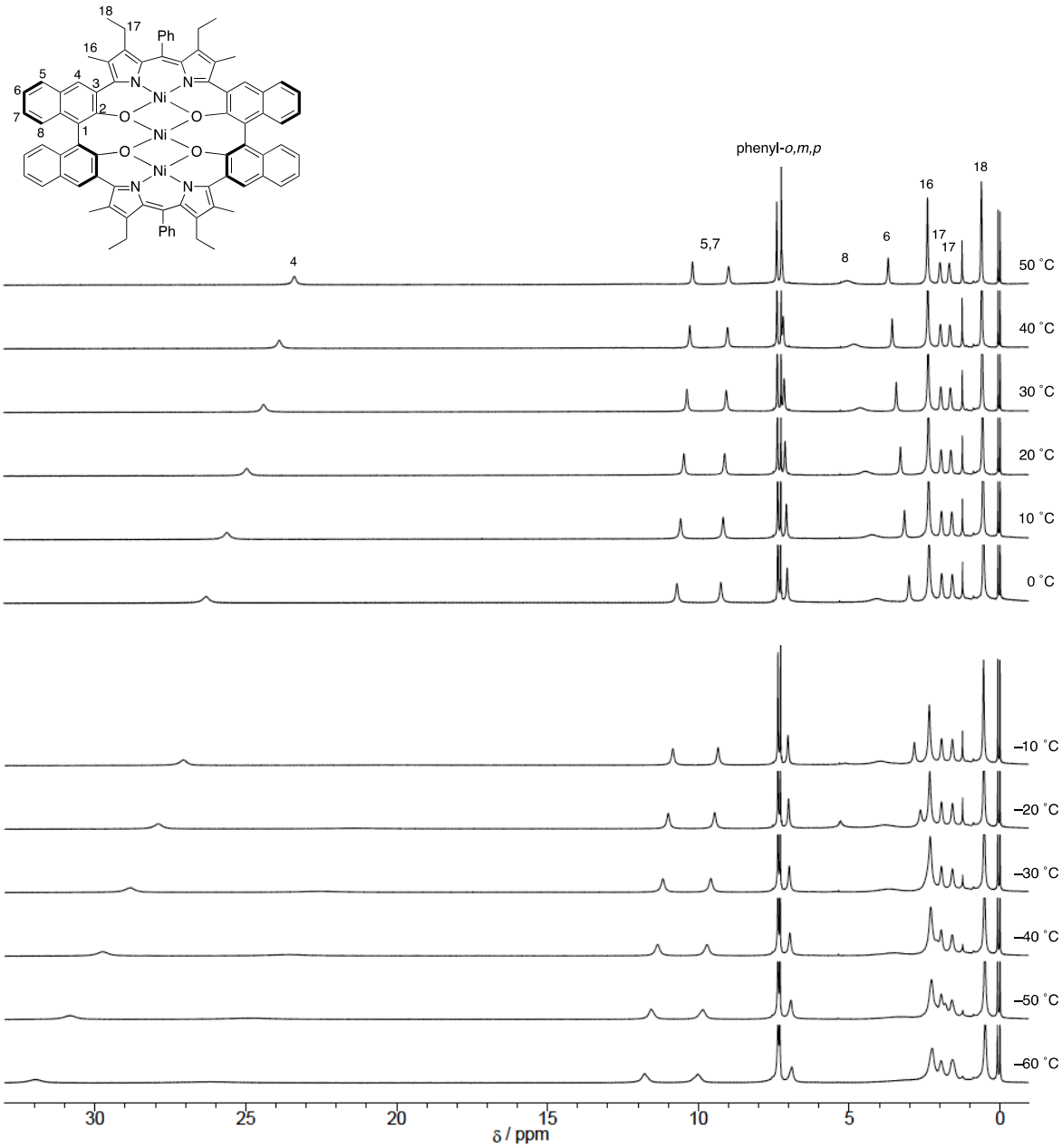

Figure S6. Variable temperature ^{1}H NMR spectra of the Ni_3 complex of bis(binaphthol)tetrapyrrole ((*S*)-**6a**). 50 ˚C ~ 0 ˚C (top) and –10 ˚C ~ –60 ˚C (bottom).

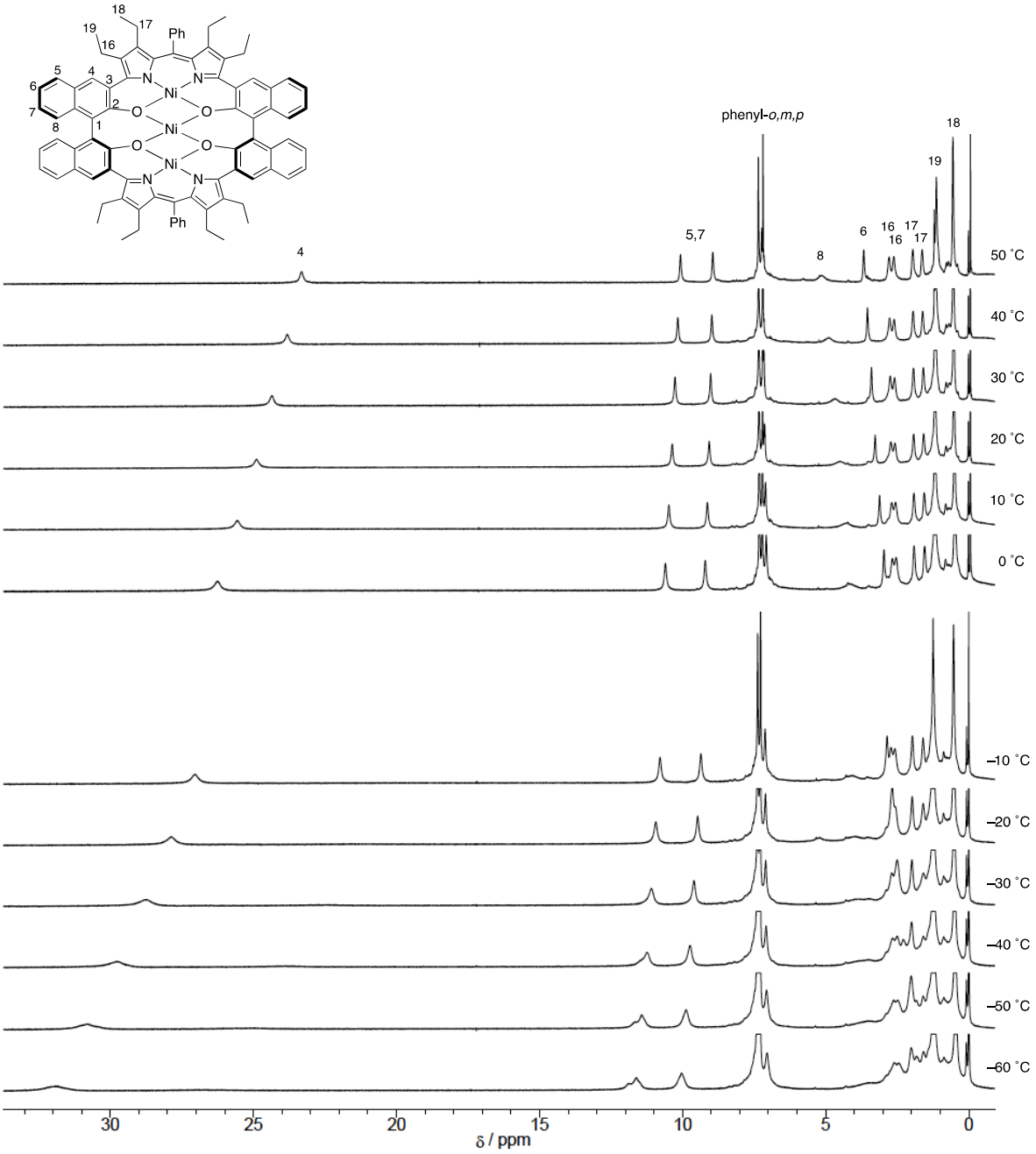

Figure S7. Variable temperature ^{1}H NMR spectra of the Ni_3 complex of bis(binaphthol)tetrapyrrole ((*S*)-**6b**). 50 ˚C ~ 0 ˚C (top) and –10 ˚C ~ –60 ˚C (bottom).

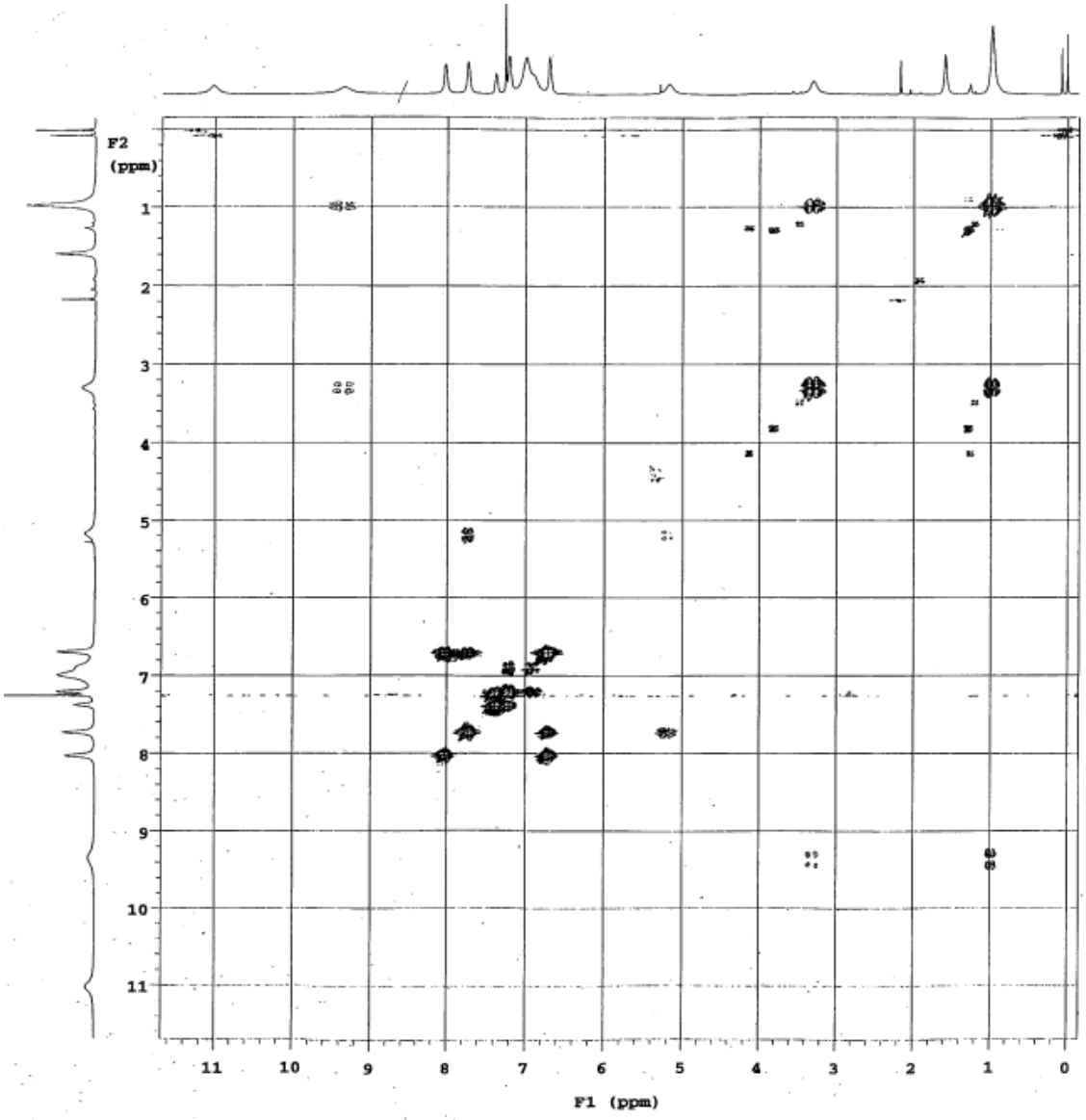

Figure S8. 2D COSY spectrum of the Cu_3 complex of bis(binaphthol)tetrapyrrole ((*S*)-**5a**) at 313 K.

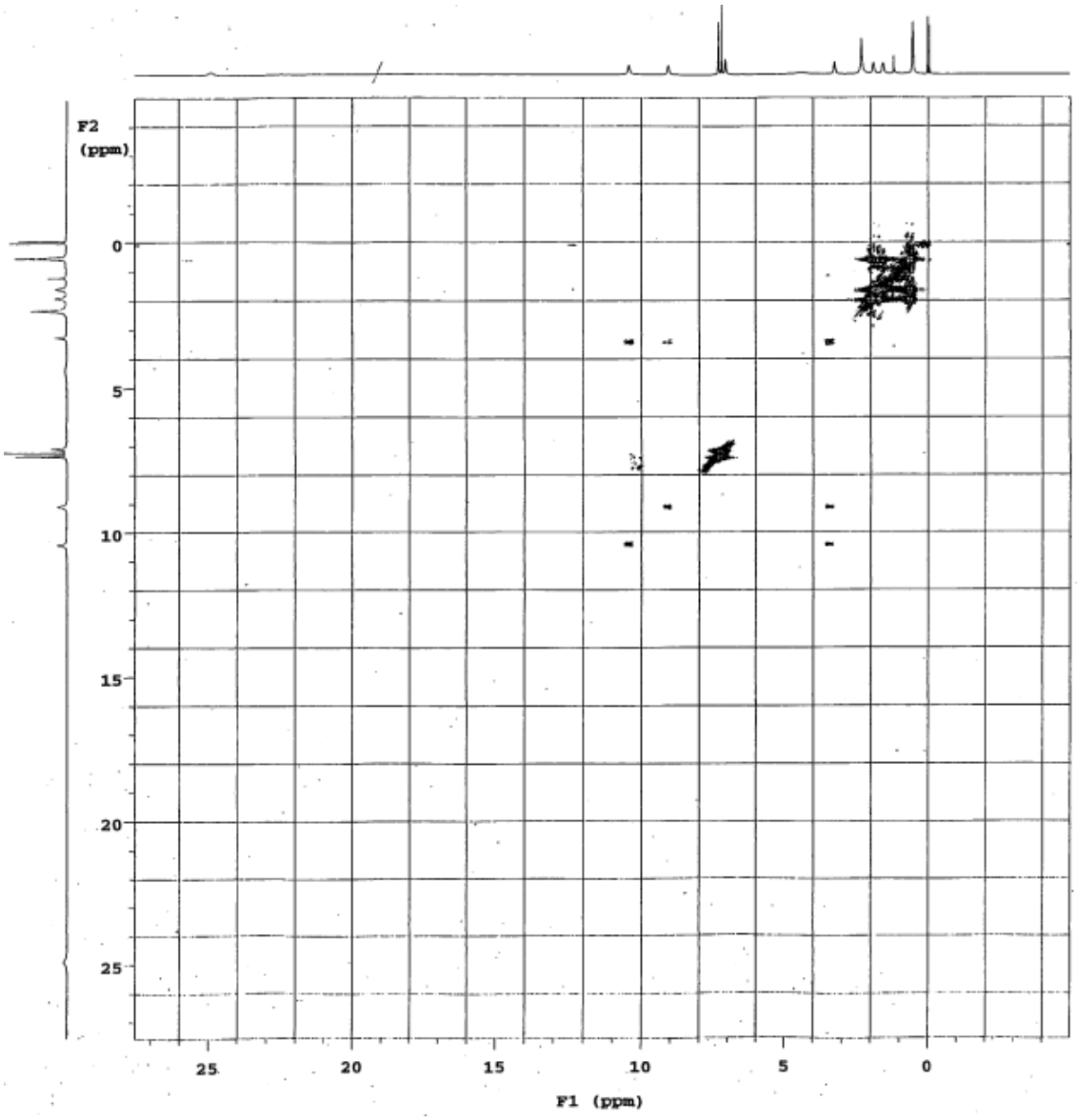

Figure S9. 2D COSY spectrum of the Ni_3 complex of bis(binaphthol)tetrapyrrole ((*S*)-**6a**) at 293 K.

UV-Vis and CD spectra

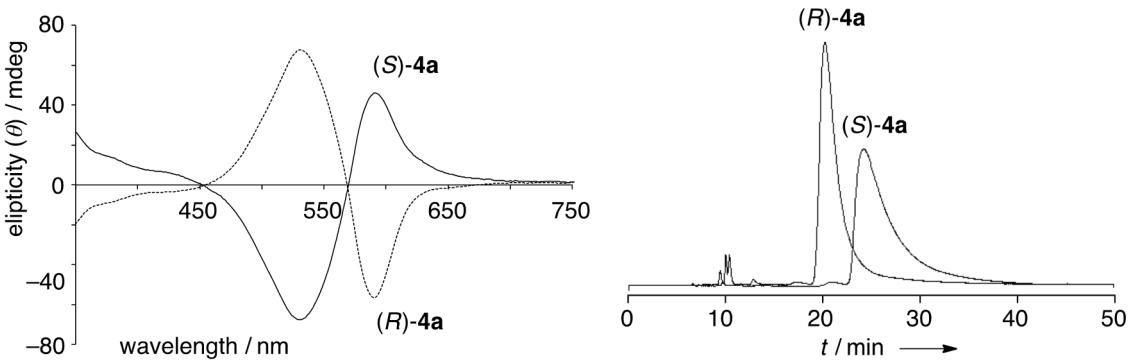

Figure S10. CD spectra of (*R*)-**4a** and (*S*)-**4a** in CH_2Cl_2 (left) and HPLC traces of (*R*)-**4a** (retention time 20.05 min) and (*S*)-**4a** (retention time 24.0 min) (right). Column: CHIRALCEL®-IA; Eluent: hexane/EtOH = 100/1; Flow: 1.0 ml/min; UV-vis detection at 575 nm.

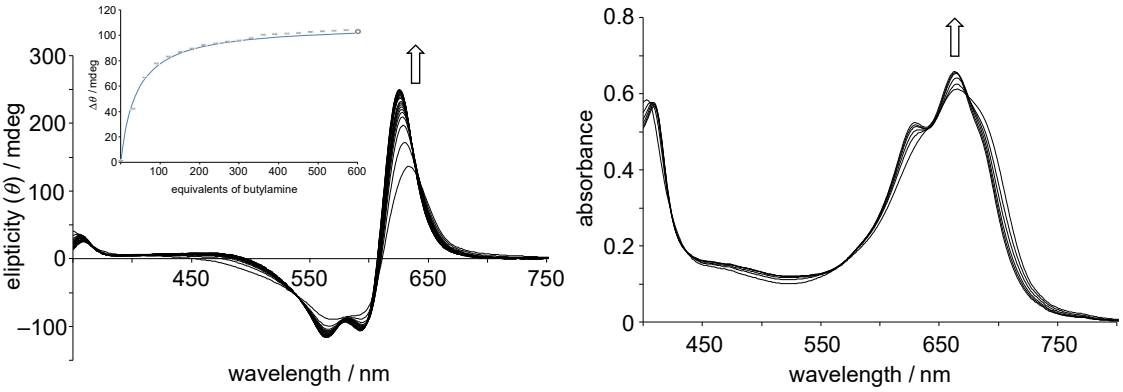

Figure S11. CD (left) and UV-Vis (right) spectral changes of (*S*)-**5a** (7.89 μM in CH_2Cl_2) by adding CH_2Cl_2 solution of butylamine (47.4 mM) at 25 °C. Inset: The observed CD intensity changes at 630 nm with molar equivalents of $BuNH_2$ and a titration curve (blue) simulated by one-to-one binding isotherm ($K = 3.2 \times 10^3\ M^{-1}$).

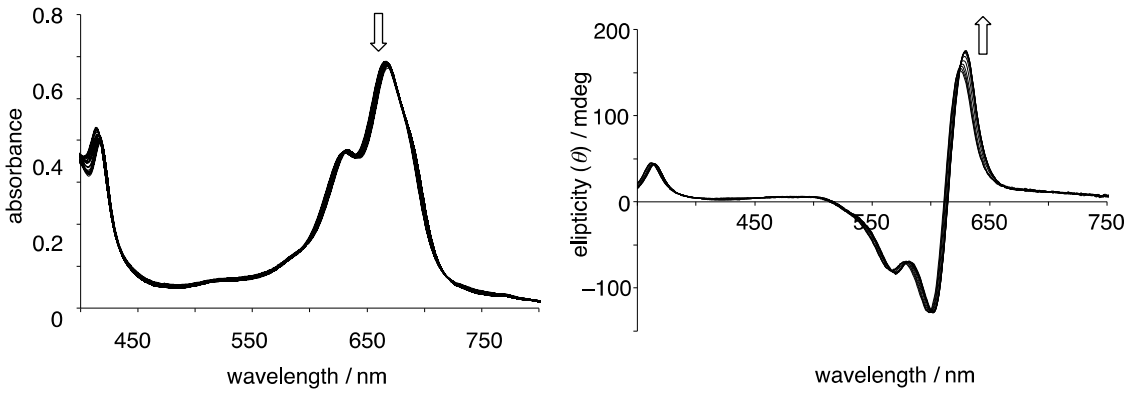

Figure S12. CD (left) and UV-Vis (right) spectral changes of (*S*)-**6a** in CH_2Cl_2 upon addition of butylamine (0 ~ 2.5 equiv).

X-ray and DFT data

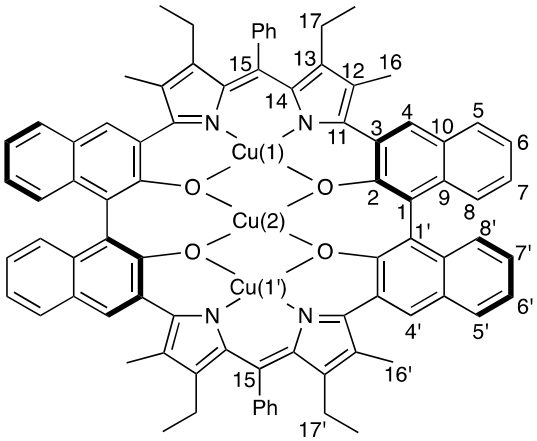

Table S1. Cu-to-H distances (Å) in the X-ray structure of (*S*)**-5a**

	Cu(1)	Cu(2)	Cu(1′)
naphthyl-4,4′-H	5.180, 5.117	5.798, 5.964	7.638, 7.731
naphthyl-5,5′-H	7.224, 7.211	7.129, 7.239	8.196, 8.301
naphthyl-6,6′-H	8.717, 8.742	8.135, 8.010	8.431, 8.436
naphthyl-7,7′-H	8.588, 8.598	7.309, 7.410	7.168, 7.178
naphthyl-8,8′-H	6.772, 6.859	5.364, 5.397	5.311, 5.348
	5.455, 5.343	6.847, 6.559	8.851, 8.761
pyrrole-16,16′-CH_3	5.735, 5.836	7.261, 7.346	9.344, 9.636
	5.964, 5.907	7.847, 7.643	10.101,10.063
pyrrole-17,17′-CH_2	5.457, 5.741	8.137, 8.088	10.988, 10.804
	5.591, 5.998	8.334, 8.461	11.104, 11.052
phenyl-*o,o′*-H	5.159, 5.501	7.883, 8.315	10.712, 11.163

[1] Distances from the specific hydrogens to three Cu atoms, Cu(1), Cu(2), and Cu(1′).

Table S2. Structural data (distance (Å) and angle (°)) of the Cu_3O_4 core of (*S*)-**5a** obtained by X-ray crystallography and theoretical DFT calculations

	X-ray	DFT (S = 1/2)		DFT (S = 3/2)	
		B3LYP	ωB97XD	B3LYP	ωB97XD
Cu(1)–O(1),O(1′ or 3)	1.877	1.946, 1.927	1.924	1.941	1.925
Cu(1)–O(2),O(2′ or 4)	1.893	1.947, 1.927	1.929	1.941	1.930
Cu(2)–O(1),O(1′ or 3)	1.949	2.001, 2.007	1.952	1.986	1.955
Cu(2)–O(2),O(2′ or 4)	1.922	2.005, 2.009	1.952	1.986	1.956
Cu(2)–Cu(1),Cu(1′ or 3)	2.910	2.887, 3.055	2.930	2.922	2.911
Cu(1)–Cu(2)–Cu(1′ or 3)	174.7	180	179.7	180	179.6

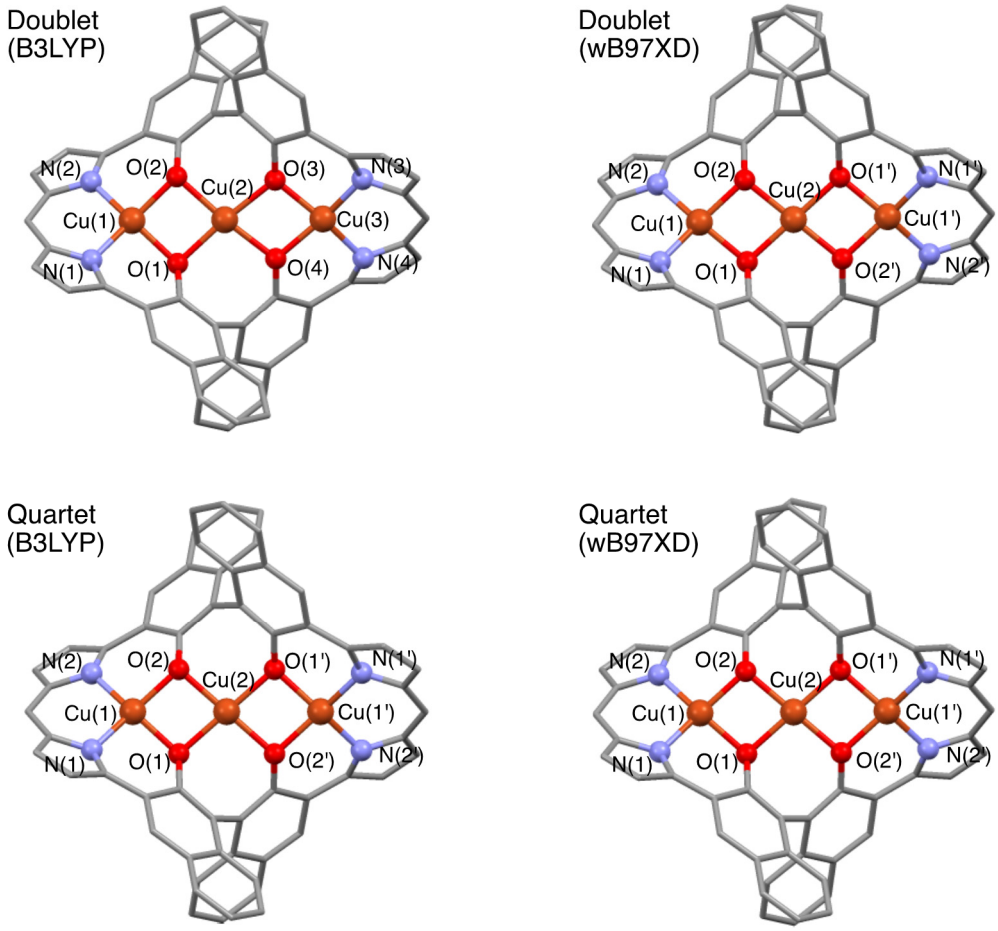

Figure S13. DFT-calculated structure of (*S*)-**5a** of doublet (top) and quartet (bottom) using B3LYP functional (left) and wB97XD functional (right). Peripheral alkyl groups and meso-phenyl groups were omitted for clarithy.

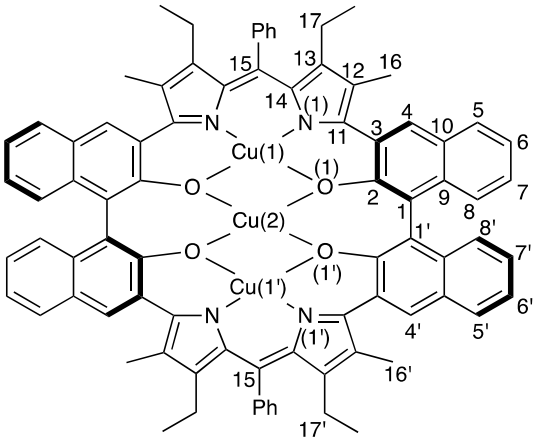

Table S3. Spin density of (*S*)-**5a** calculated by DFT (6-31G(d), LANL2DZ/*ω*B97XD)

	S = 1/2		S = 3/2	
Cu(1), Cu(1′)	0.5977		0.6083	
Cu(2)	–0.6169		0.6366	
naphthyl-O(1),O(1′)	–0.0018	–0.0032	0.1428	0.1453
dipyrrin-N(1),N(1′)	0.1061	0.1051	0.1099	0.1093
naphthyl-C(1),C(1′)	–0.0160	–0.0183	0.0237	0.0262
naphthyl-C(2),C(2′)	0.0119	0.0133	–0.0111	–0.0128
naphthyl-C(3),C(3′)	–0.0078	–0.0085	0.0120	0.0128
naphthyl-C(4),C(4′)	0.0061	0.0069	–0.0082	–0.0092
naphthyl-C(5),C(5′)	0.0047	0.0053	–0.0052	–0.0058
naphthyl-C(6),C(6′)	–0.0060	–0.0067	0.0066	0.0073
naphthyl-C(7),C(7′)	0.0043	0.0048	–0.0048	–0.0053
naphthyl-C(8),C(8′)	–0.0054	–0.0060	0.0063	0.0070
naphthyl-C(9),C(9′)	0.0068	0.0075	–0.0066	–0.0074
naphthyl-C(10),C(10′)	–0.0073	–0.0081	0.0082	0.0091
pyrrole α-C(11),C(11′)	0.0026	0.0029	–0.0006	–0.0013
pyrrole β-C(12),C(12′)	0.0034	0.0036	0.0047	0.0053
pyrrole β-C(13),C(13′)	0.0072	0.0072	0.0067	0.0062
pyrrole α-C(14),C(14′)	–0.0029	–0.0029	–0.0029	–0.0030
meso-like-C(15)	0.0010		0.0034	
methyl-C(16),C(16′)	0.0010	0.0010	0.0009	0.0009
methylene-C(17),C(17′)	0.0004	0.0003	0.0005	0.0004

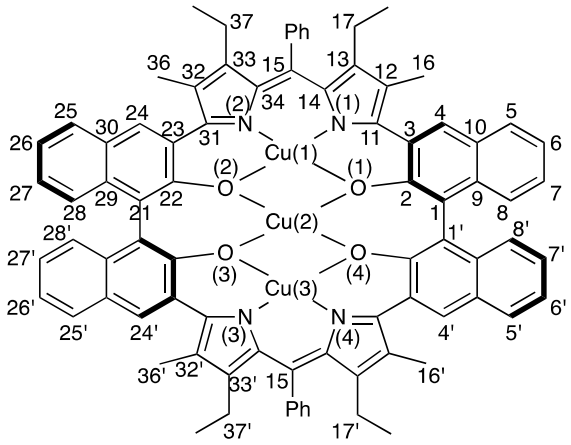

Table S4. Spin density of (*S*)-**5a** calculated by DFT (6-31G(d), LANL2DZ/B3LYP).

	S = 1/2		S = 3/2	
Cu(1)	0.558750		0.565394	
Cu(2)	0.006671		0.518978	
Cu(3)	–0.000749		0.565394	
naphthyl-O(1),O(3)	0.082622	–0.000766	0.158765	0.158795
naphthyl-O(2),O(4)	0.083406	–0.000694	0.158741	0.158769
dipyrrin-N(1),N(3)	0.116518	0.000020	0.116626	0.116647
dipyrrin-N(2),N(4)	0.117220	0.000034	0.116624	0.116637
naphthyl-C(4),C(4′)	–0.000631	0.000052	–0.008633	–0.008638
-C(24),C(24′)	–0.000871	0.000044	–0.008626	–0.008633
naphthyl-C(5),C(5′)	0.000223	0.000025	–0.007438	–0.007422
-C(25),C(25′)	0.000149	0.000015	–0.007423	–0.007439
naphthyl-C(6),C(6′)	–0.000026	–0.000024	0.014233	0.014241
-C(26),C(26′)	0.000054	–0.000006	0.014222	0.014236
naphthyl-C(7),C(7′)	–0.000064	0.000055	–0.007992	–0.007998
-C(27),C(27′)	–0.000161	0.000049	–0.007985	–0.007993
naphthyl-C(8),C(8′)	0.000577	–0.000055	0.013538	0.013547
-C(28),C(28′)	0.000672	–0.000044	0.013528	0.013542
pyrrole β-C(12),C(12′)	0.005894	0.000065	0.006143	0.006149
-C(32),C(32′)	0.005879	0.000054	0.006141	0.006141
pyrrole β-C(13),C(13′)	0.006522	0.000069	0.009656	0.009648
-C(33),C(33′)	0.006017	0.000090	0.009667	0.009655
methyl-C(16),C(16′)	0.000989	–0.000004	0.000947	0.000947
-C(36),C(36′)	0.000998	–0.000003	0.000947	0.000948
methylene-C(17),C(17′)	0.000487	–0.000010	0.000288	0.000289
-C(37),C(37′)	0.000523	–0.000012	0.000288	0.000288